Sustainable Materials and Technologies 42 (2024) e01146

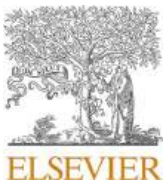

Contents lists available at ScienceDirect

Sustainable Materials and Technologies

journal homepage: www.elsevier.com/locate/susmat

Stable and reusable electrospun bio-composite fibrous membranes based on PLA and natural fillers for air filtration applications

Roberto Scaffaro [a,b,*], Maria Clara Citarrella [a,b]

[a] Department of Engineering, University of Palermo, Viale delle Scienze, ed. 6, 90128 Palermo, PA, Italy
[b] INSTM, Consortium for Materials Science and Technology, Via Giusti 9, 50125 Florence, Italy

ARTICLE INFO

Keywords:
Biocomposite
Natural filler
PLA
Air filtration
PM capture
Electrospinning

ABSTRACT

Today, air pollution due to fine dust is one of the most critical environmental challenges. To mitigate the potential further environmental impact of air filtration devices, it is essential to explore the use of biodegradable polymers combined with natural fillers, preferably sourced from waste materials, to develop stable, reusable and UV-resistant air filters suitable for outdoor applications. In this work, composite fibrous membranes based on polylactic acid (PLA) and natural fillers were prepared via electrospinning and tested for air filtration applications. Air filtration performances were evaluated at different flow rates, temperature and humidity condition, aiming to simulate outdoor conditions. The addition of 10 wt% of *Opuntia Ficus Indica* (OFI), *Posidonia Oceanica Leaves* (POL) or lignin (LIG) particles to PLA solution led to a decrease in fibers diameter increasing membranes filtration performances. PLA/OFI, PLA/POL and PLA/LIG composite membranes exhibited filtration efficiencies of 97.2 %, 99.4 %, 99.6 % for PM_3 at a flow rate of 32 L/min, and pressure drops of 114, 103, 105 Pa, respectively. The membranes demonstrated stability maintaining good filtration efficiency across different environmental conditions and after multiple reuse cycles. The addition of OFI and LIG powders also provided effective UV resistance, crucial for ensuring the longevity and performance of air filters exposed to outdoor conditions. These findings underscore the potential of these biodegradable composite membranes for sustainable indoor and outdoor air filtration solutions.

1. Introduction

In recent years, environmental pollution has become an increasingly prominent focus of scientific research and public concern [1,2]. Air pollution and plastic waste disposal have become two of the most closely monitored global problems. The COVID-19 pandemic, in particular, has highlighted significant problems associated with both indoor and outdoor air pollution and waste management [3,4]. The spread of the virus has demonstrated how air pollution can promote and boost the transmission of respiratory diseases. Simultaneously, the pandemic has led to a significant increase in plastic waste production, largely due to the disposal of traditional filter membranes used in personal protective equipment, air purifiers and other similar devices [5]. Actually, commercial filters are predominantly made from melt-blown polypropylene fibers. These membranes exhibit several limitations [6,7]: i) their morphological structure, characterized by fibers with relatively large diameters, presents large pore sizes that do not allow for high filtration efficiencies, particularly for small particulate matter; ii) their filtration performances deteriorates rapidly over time; iii) they are non-biodegradable, leading to plastic and microplastic pollution when dispersed into the environment. These aspects highlight the urgent need to address environmental challenges related to pollution with innovative and sustainable solutions that can be reused multiple times before being composted when their efficiency no longer meets the required standards [8,9]. To achieve these ambitious goals, it is important to develop fibrous membranes based on biodegradable polymers capable of being reused several times and eventually composted.

For outdoor air filtration applications it is crucial that the membranes remain stable under various climatic conditions and resist UV exposure. Outdoor environments subjects filtration membranes to fluctuating temperatures, humidity, and prolonged UV radiation, which can degrade the material and compromise filtration efficiency. UV-resistant membranes ensure prolonged operational life and consistent performance, reducing the need for frequent replacements and minimizing environmental impact [10].

Furthermore, developing effective outdoor air filtration devices is

* Corresponding author at: Department of Engineering, University of Palermo, Viale delle Scienze, ed. 6, 90128 Palermo, PA, Italy.
E-mail address: roberto.scaffaro@unipa.it (R. Scaffaro).

https://doi.org/10.1016/j.susmat.2024.e01146
Received 25 August 2024; Received in revised form 2 October 2024; Accepted 9 October 2024
Available online 11 October 2024

important for protecting public health in urban areas where pollution levels are high and in environments where industrial activities release significant amounts of pollutants. Such devices can help mitigate the adverse effects of air pollution, providing cleaner air and contributing to overall environmental quality. Specifically, implementing air filtration panels near schools, parks, and other public spaces in heavily trafficked or industrialized areas can create healthier environments for children and the general public, reducing exposure to harmful pollutants and improving community health.

In recent years, electrospun fiber filters made from poly(lactic acid) (PLA) have been extensively developed thanks to its' reputation for being an environmentally friendly polymer with good biodegradability, satisfactory mechanical properties and non-toxic degradation products [11–17]. Moreover, it has been proven that, by embedding particles of different nature in PLA fibers, it is possible to enhance PM capture. Natural halloysite nanotubes (HNTs) and silver phosphate (Ag_3PO_4) have been incorporated into PLA fibers, leading to an increase in the electrostatic interaction with PMs and extending the service life of the membranes [18]. Similar results have been obtained by adding ZIF-8 nanocrystals and carbon nanotubes [19] or dielectric TiO_2 nanocrystals [20] to PLA nanofibers. Additionally, it is possible to enhance the filtration properties of PLA membranes using natural filler. For example, diatom frustules (DFs) have been added to PLA solution, resulting in electrospun composites membranes. The presence of DFs lead to smaller fiber diameter and pores, which improved filtration efficiency [5]. The addition of calendula extract has also modified the morphology and porous structure of the PLA fibers, enhancing the filtration efficiency and providing UV protection to the membrane [21].

Electrospinning is increasingly recognized as one of the most versatile and efficient techniques for fabricating fibrous membranes [22]. An electrospinning apparatus typically comprises a spinneret, a high-voltage system, and a grounded collector. During the electrospinning process, an electrostatic force manipulates the polymeric solution, pulling fibers as it flows. When this force surpasses the liquid's surface tension, droplets from the spinneret deform into a cone shape known as a "Taylor cone" originating the fibers that are then collected by a grounded collector [23]. The use of electrospun membranes in air filtration applications is particularly promising. The fine fibrous structure of electrospun mats provides an extensive surface area, which may enhance the capture efficiency of particles, including pollutants, allergens, and pathogens [24,25].

Traditionally, agricultural and vegetable waste biomass is often discarded or underutilized, contributing to environmental pollution and resource wastage [26]. The use of this biomass in combination with biodegradable polymers for the production of functional devices for pollutant removal not only provides an effective attempt at mitigating environmental hazards but also contributes to the circular economy by transforming waste into value-added products [27–29].

In this work, stable, reusable and UV-resistant bio-composite fibrous membranes were fabricated, through electrospinning, by adding 10 wt% of Opuntia Ficus Indica (OFI), *Posidonia Oceanica* Leaves (POL) or lignin (LIG) powders to the PLA solution. The PLA/POL and PLA/LIG membranes showed a notable reduction in fiber diameter due to the increased conductivity of the solutions. Furthermore, the incorporation of lignin in the membranes improved their electroactivity. The PLA/OFI, PLA/POL, and PLA/LIG composite membranes demonstrated excellent filtration performance at a flow rate of 32 L/min, especially for PM_3. Additionally, the composite membranes demonstrated stability maintaining good filtration efficiency across different environmental conditions and were able to be reused for at least five washing cycles while maintaining their fibrous structure and good filtration efficiency. Crucially, the addition of OFI and LIG powders to PLA fibers provided UV protection, making these membranes ideal for outdoor air filtration applications. This study underscores the potential of these biodegradable composite membranes as a starting point to develop sustainable and durable outdoor air filtration solutions to be used as part of panels in public spaces near high-traffic and industrialized areas to reduce exposure to air pollutants and improving community health.

2. Experimental section

2.1. Materials and methods

2.1.1. Materials

Polylactic acid (PLA, 2003D, Mw = 98 kDa) was purchased at NatureWorks. Acetone (Ac), chloroform (Chl), deionized water and other chemicals of analytical grade were purchased from Sigma-Aldrich. Kraft lignin (LIG) was obtained from black liquor using the Lignoboost technology. The cladodes from *Opuntia Ficus Indica* (OFI; cellulose: 20 %, lignin: 3 %, hemicellulose: 48 %, ashes: 20 %, other: 9 %) were supplied by Bio Ecopuntia (Italy), while scraps of *Posidonia Oceanica* leaves (POL; cellulose: 31 %, lignin: 29 %, hemicellulose: 26 %, ashes: 10 %, other: 4 %) were collected on the Mondello coast in Palermo, Italy.

2.1.2. Preparation of PLA/fillers dispersions and membranes

Firstly, OFI cladodes and POL scraps were washed in water at room temperature and dried in an oven at 60 °C for 48 h. The two scraps were then chopped and roughly ground for 3 min. Subsequently, OFI, POL and LIG particles were ball-milled (Retsch MM 500 nano, Germany) for 30 min at 20 Hz aiming to obtain micrometric powder. PLA solution (10 wt %) was prepared using Chl/Ac mixture (2:1 ratio). After the PLA was completely dissolved, 1, 3, 5, 10 and 15 wt% (with respect to PLA mass) of OFI, POL and LIG powders, were separately dispersed in the PLA solution (Fig. 1a, b) keeping them under magnetic stirring at 25 °C overnight. Preliminary electrospinning tests were performed on all the composites PLA dispersion. For the dispersion containing 1, 3, 5 and 10 wt% of the natural particles, no clogging of the needle (1 mm diameter) was observed during the electrospinning process. However, for 15 wt% dispersions, the spinning process experiences frequent interruptions due to the formation of agglomerates of natural particles in the needle, especially for POL containing dispersion. Ultimately, 10 wt% composite solutions were selected and labeled as PLA/OFI, PLA/POL and PLA/LIG, respectively, for two key reasons: i) maximize the presence of natural particles in the filtering membranes aligns with sustainability objectives, as it allows for the incorporation of a larger amount of waste material into the membrane; ii) the particles act as accumulation points for pollutants, so increasing their content contributes to enhanced filtration efficiency and overall membrane performance. Moreover, the presence of the fillers potentially increases fibers roughness and the chances of PMs to be caught on them [30].

The production of composite fibrous membranes was carried out using the electrospinning technique (Fig. 1c) with a conventional equipment consisting of a syringe pump and a high voltage power supply (Linari Engineering-Biomedical Division, Pisa, Italy). During the spinning process, the voltage applied was 15 kV, the inner diameter of the needle was 1 mm and the distance from the needle to the drum was 15 cm. The flow rate was 0.3 mL/h, and the drum speed was 200 rpm. The temperature during processing was kept at 23 ± 2 °C, and the relative humidity of the air was 50 ± 5 %. The obtained fibrous membranes were then dried at room temperature for 24 h to remove any residual solvent. According to the starting dispersions, the membranes were labeled PLA, PLA/OFI, PLA/POL and PLA/LIG (Fig. 1c).

2.2. Characterizations

2.2.1. Natural fillers and composite membranes morphology

Scanning electron microscope (SEM, Phenom ProX, Phenom-World, The Netherlands) was used in order to observe the morphology of the natural fillers and of the nanofibers before and after the filtration test adopting the operative conditions already used in our previous work [12] and briefly reported in SI. Fibers diameter size distribution was measured using ImageJ software equipped with the DiameterJ plugin

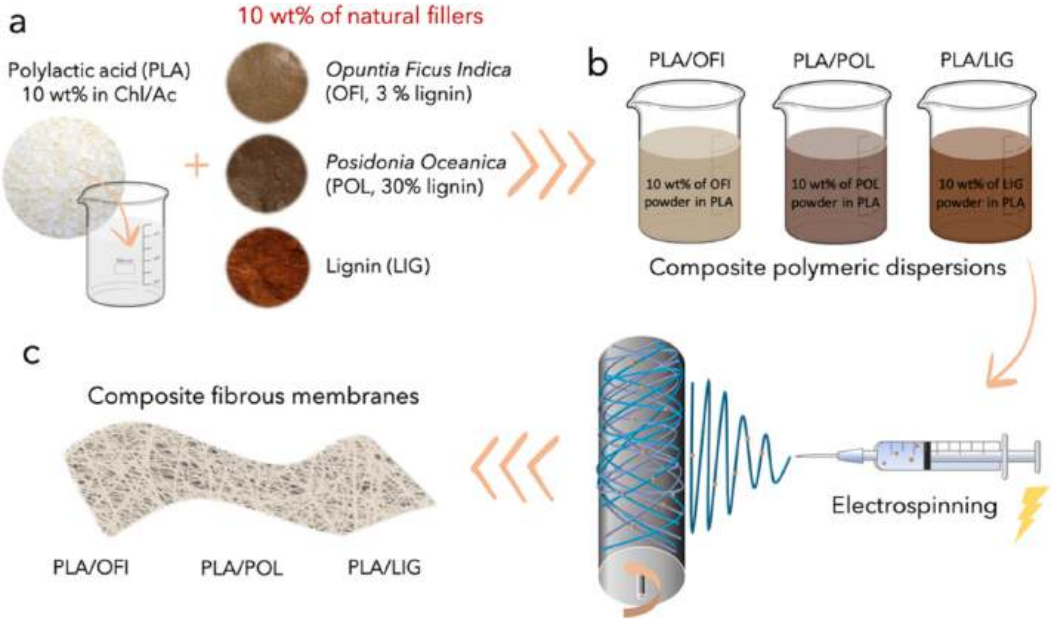

Fig. 1. Schematic illustration for the preparation of the composite membranes: (a) preparation of the composite dispersions; (b) composition of PLA/OFI, PLA/POL, and PLA/LIG dispersions; (c) fabrication of PLA/OFI, PLA/POL, and PLA/LIG composite fibrous membranes via electrospinning.

following the same procedure already reported in our previous work [12] and briefly reported in SI.

2.2.2. Dispersions properties

Rotational rheometer (ARES-G2, TA Instruments, New Castle, DE, USA) and conductivity meter (Xylem, Weilheim in Oberbayern, Germany) were used to test the viscosity and conductivity of the four polymeric dispersions respectively. The rheological properties were investigated following the same procedure already reported in our previous work [12] and briefly reported in SI.

2.2.3. Composite membranes characterizations

Chemical and structural characterization of membranes surfaces were assessed by FT-IR/ATR analysis, carried out by using Perkin-Elmer FT-IR/NIR Spectrum 400 spectrophotometer. The absorbance spectra were recorded in the wavenumber range 4000–400 cm^{-1}.

The mechanical performance of the membranes was investigated by carrying out tensile tests on a laboratory dynamometer (Instron model 3365, UK) equipped with a 1 kN load cell. The relative procedure is reported in SI.

2.2.4. Air filtration performance

Air filtration performance of the composites membranes was evaluated on a homemade filtration test system by simulating a polluted air environment. In Fig. 2 a schematic representation of the filtration test system is depicted. Chamber (A) and chamber (B) represent upstream and downstream chambers respectively, while the testing membrane is placed in between. More in detail, to evaluate the air filtration performance, PLA, PLA/OFI, PLA/POL, PLA/LIG membranes of 100 μm thickness were fixed into a filter holder in the middle of the filtration setup. Burning incense was used to generate the particles (PMs), with particles size ranging from 0.3 μm to 3 μm, aiming to simulate a polluted air environment. The produced particles were delivered through the membranes by inject air at different flow rate (10, 32, 65, 85 L/min) in the upstream chamber (A). The particle counters (SEK-SVM4x, Sensirion, Switzerland) were used to determine the particle concentrations in the two chambers i.e. in upstream (A) and downstream (B) of the tested membrane. The micromanometer (SDP810-500PA, Sensirion, Switzerland) was used to measure the air resistance of the filter (ΔP), i.e., the difference between upstream and downstream of the test membrane. The filtration efficiency of PMs (η) was calculated according to Eq. (1):

$$\eta = \left(1 - \frac{C_1}{C_2}\right) \times 100 \quad (1)$$

where C_1 and C_2 represented the PM concentration respectively in the

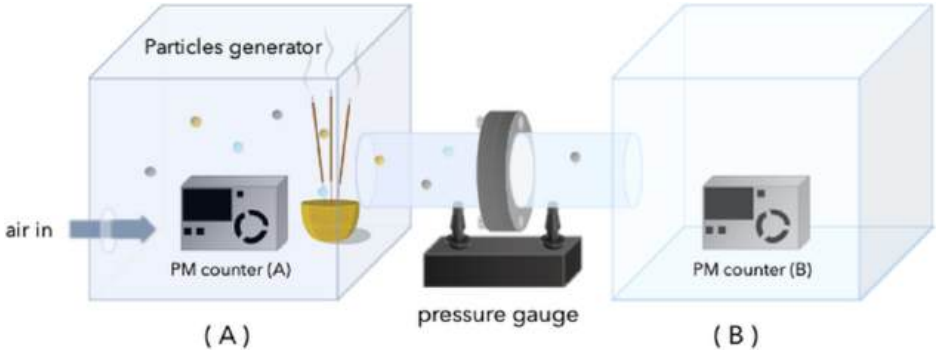

Fig. 2. Schematic illustration for the implemented homemade filtration test. Chamber (A) and chamber (B) represent upstream and downstream chambers respectively.

downstream airflow and upstream airflow through the tested membrane. The PMs counting concentration was measured for 2 min and each group of membranes was tested in triplicate. Aiming to comprehensively evaluate of the filtration performance of the membranes, the quality factor (QF) of the filtering membranes was calculated according to Eq. (2):

$$QF = -\frac{ln(1-\eta)}{\Delta P} \quad (2)$$

where η represents the filtration efficiency and ΔP represents the pressure drop.

Air filtration performances of the membranes were monitored at different temperatures (35, 25, 15 °C) and relative humidity (RH, 30, 60, 80 %) conditions. Air conditioners and a humidifier were used to control and varying the environment temperature and humidity during the experiments. Moreover, the filtration efficiencies were tested for five cycles aiming to evaluate their potential reusability. After each filtration cycle the membranes were washed with a 70:30 water/ethanol mixture, aiming to remove the PM, and let them air dry for 2 h.

2.2.5. UV protection performance test

UV–visible spectrophotometer (model UVPC 2401, Shimadzu Italia s.r.l., Milan, Italy) was utilized to measure the UV transmittance of the filtering membranes, with test wavelengths ranging from 200 to 400 nm. The UV protection ability of the natural fillers incorporated in the membranes was determined by comparing the fiber morphology (SEM analysis) before and after irradiation with an ultraviolet lamp (OSRAM, 315–400 nm UVA and 280–315 nm UVB), with an irradiation distance of 1 cm and an irradiation time of 2, 4 and 8 h in a climatic chamber set at 25 °C.

2.2.6. Statistical analysis

Data obtained underwent statistical analysis with an unpaired Student *t*-test using GraphPad Prism 9. Statistical significance was attributed to differences between datasets when the *p*-value obtained was lower than 0.05 (**** $p < 0.0001$; *** $p < 0.001$; ** $p < 0.01$).

3. Result and discussion

3.1. Morphology of natural particles

The morphology of OFI, POL and LIG particles, after the ball-milling process, was analyzed by SEM and show in Fig. 3a-c, while the respective particles size distribution, in terms of equivalent diameter, are reported in Fig. 3a‘-c’.

OFI and LIG particles (Fig. 3a, c) are both characterized by a fairly spherical shape and an average diameter of about 2.5 μm (Fig. 3a‘, c’). As desired, the use of ball milling allowed obtaining powders characterized by particles size in the range of few micrometer, likely facilitating the electrospinning process. However, while LIG particles are quite homogeneous in dimensions and shape, OFI powder also present few bigger and elongated particles. On the other hand, POL particles are less inclined to be reduced into spherical particles of a few micrometers during ball milling process, as shown in Fig. 3b. In this case, irregularly shaped particles with an average diameter of about 8 μm (Fig. 3b‘) are obtained, but some particles as large as 100 μm can be also noted. Differently from OFI and LIG ones, POL particles are, furthermore, characterized by a porous structure with deep channels along their entire surface, as is possible to notice in Fig. S1. However, it can be concluded that OFI, POL and LIG powders seems to be all dimensionally compatible with electrospinning process.

3.2. Electrospun dispersions properties

The properties of the electrospun polymeric dispersions were investigated and results are reported in Fig. 4. Generally, in fact, differences in the composition of the spinning solution can affect their viscosity and this, in turn, can modify the morphology of the electrospun fibers [5,21]. Higher viscosity solutions typically result in thicker and more uniform fibers. This is because higher viscosity indicates greater polymer chain entanglement, which resists the stretching forces during electrospinning, leading to larger diameter fibers. Moreover, the increased viscosity stabilizes the jet formed during electrospinning, reducing fluctuations that can cause variations in fibers diameter.

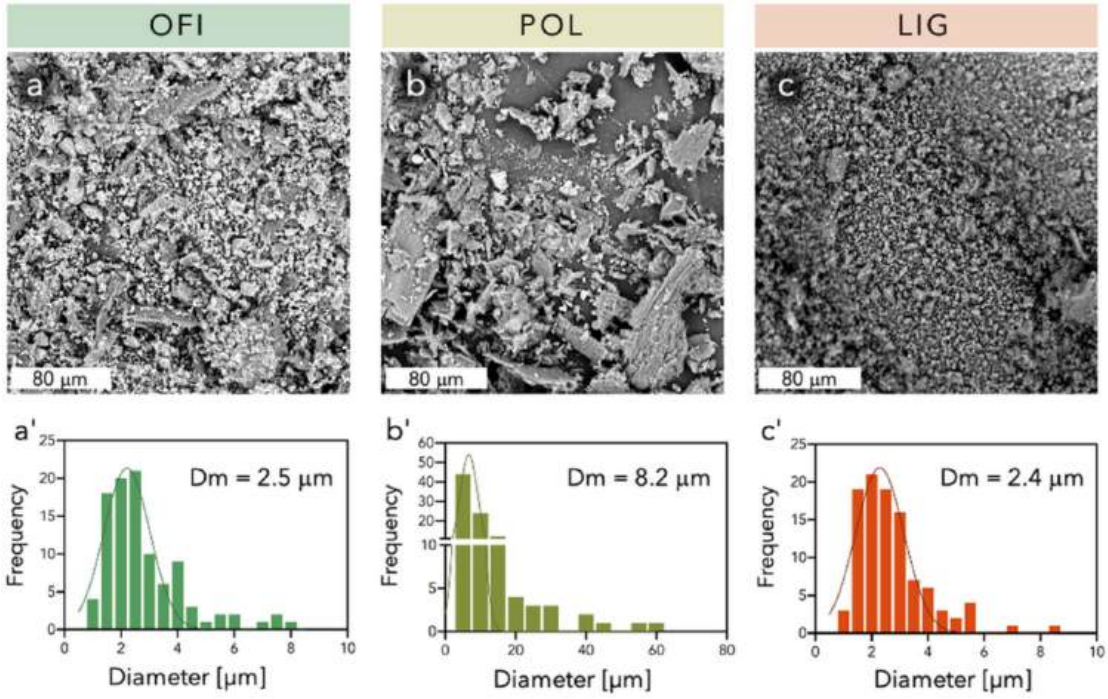

Fig. 3. SEM images and size distribution of OFI (a, a’), POL (b, b’), LIG (c, c’) particles respectively.

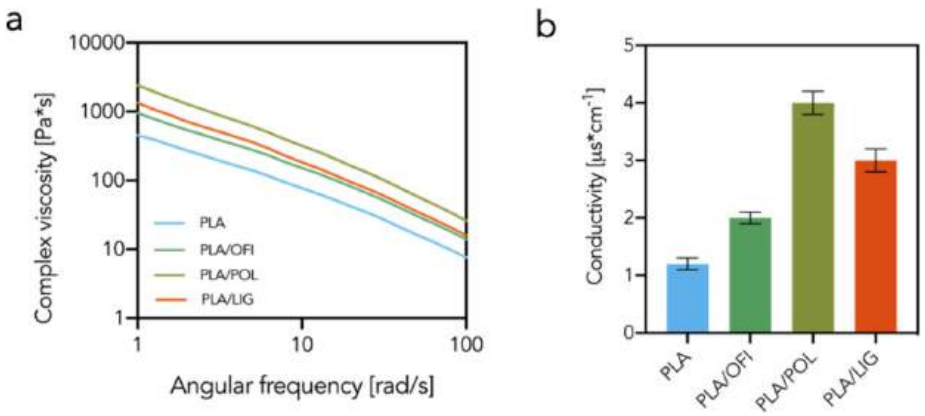

Fig. 4. Complex viscosity (a) and conductivity (b) of electrospun polymeric dispersions.

Conversely, lower viscosity solutions tend to produce thinner fibers.

As regards rheological tests, neat PLA shows a pronounced non-Newtonian behaviour across the entire frequency range (Fig. 4a). When natural particles were added to the PLA solution, a significant increase in viscosity value across the entire frequency range is observed, while the overall rheological behaviour remained unchanged for all the composite dispersions. However, the presence of POL powder induces a higher increase in viscosity value if compared to the other two fillers. This apparently strange behaviour can be attributed to the porous structure of the larger POL particles (Fig. 3b and Fig. S1), which enhances the interfacial interactions between the polymer and the dispersed phase. In other words, the porous POL particles provide more sites for physical interactions with PLA, contributing to the viscosity increase, as already reported in similar systems [31]. Additionally, the incorporation of solid filler particles increases the effective volume fraction of the dispersed phase in the polymer solution, leading to higher resistance to deformation and increased viscosity [32]. The more rounded shape and lower porosity of OFI and LIG particles (Fig. 3a, c) result in a reduced surface area, thus producing fewer interaction sites with the PLA chains, leading to a smaller increase in viscosity.

Conductivity of the spinning solution is another variable that can influence morphology of the fibers. Higher solution conductivity, in fact, enhances the electric charge carried by the solution, leading to greater stretching forces on the jet during spinning and thus to obtaining thinner and more elongated fibers [21]. Therefore, to verify potential effects of conductivity changes upon adding filler to PLA solution, conductivity measurements were carried out, and results are reported in Fig. 4b. The addition of all the fillers leads to an increase in conductivity if compared to the neat PLA solution (1.2 µS/cm). The PLA/POL dispersion displays the highest conductivity value, followed by PLA/LIG, reaching 4.1 and 3.3 µS/cm respectively. To address this issue, it is necessary to consider that when dispersed in polymeric systems, the molecular structure of lignin can release ions by interacting with the solvent and the polymer, increasing the electrical conductivity of the solution [32]. Moreover, the increase in electrical conductivity of the polymeric solution with the increase in lignin content has been extensively reported in the scientific literature [33]. However, the PLA/POL solution exhibited the highest conductivity among the tested systems, likely due to the to the presence of ionic compounds (e.g. residual salts) on the *Posidonia Oceanica* particles, which enhances conductive pathways in the solution [34].

3.3. Morphology of composite membranes

The electrospinning process proceeded smoothly for all the polymeric dispersion containing 10 wt% of natural particles and no clogging of the needle (1 mm diameter) was observed, even for PLA/POL that contained the largest particles. The morphology of PLA, PLA/OFI, PLA/POL and PLA/LIG membranes was observed by SEM as shown in Fig. 5a-d, while the respective fibers diameter distribution are reported in Fig. 5a"-d". PLA membranes (Fig. 5a, a') exhibit smooth and randomly oriented fibers characterized by a bimodal fiber diameter distribution with the mean values of the two modes being 1.65 µm and 2.54 µm and the average diameter of 2.21 µm (Fig. 5a"). The addition of natural fillers significantly affects fibers shape according to the different properties of the dispersions. PLA/OFI fibers appear randomly oriented with some OFI particles well distributed all over the membrane, as observed in Fig. 5b. This confirms that the particles larger than a few micrometers, which cannot be embedded inside the fibers, were easily ejected through the needle, adhering to the fibers surface and thereby being incorporated into the membrane (Fig. 5b'). The presence of these particles could be useful for improving the filtration performance of the membrane [5,21]. Moreover, the presence of OFI powder in PLA solution leads to a significative decrease in the fiber's average diameter and results in a unimodal, wide fiber diameter distribution (Fig. 5b"). This behaviour is even more pronounced in PLA/POL and PLA/LIG membranes in which the fibers average diameters reach 0.46 and 0.53 µm respectively and unimodal, narrow fiber diameter distribution is obtained for both the membranes (Fig. 5c", d"). Moreover, in PLA/POL and PLA/LIG membranes the fibers appear uniformly oriented and the presence of fibers bundles can be noted (Fig. 5c, d). In PLA/POL membranes, POL particles could be extensively identified in SEM image (Fig. 5c, c') while LIG ones seems to be almost entirely embedded into PLA fibers (Fig. 5d, d').

It is well known in the scientific literature that an increase in the viscosity of the spinning solution usually leads to the formation of fibers with a larger diameter due to the increased resistance to flow [35]. Surprisingly, this seems to be in contrast to what observed in OFI, POL and LIG composite systems. However, in this study, conductivity of the dispersions seems to predominantly influence fibers morphology. These variations in the morphology of the membranes, in fact, are compatible with the different conductivity of the relative dispersions. Higher conductivity results in stronger electrostatic forces during electrospinning, which stretch the solution more efficiently, producing thinner fibers.

3.4. Fibrous composite membranes characterizations

FTIR spectroscopy analysis was performed on the electrospun membranes and the free natural powders to characterize fibers composition, and the obtained spectra are reported in Fig. S2a-a'. The FTIR spectra of PLA/OFI, PLA/POL and PLA/LIG membranes closely resembled that of neat PLA. All the spectra show the typical PLA band of the carbonyl group (C = O) at 1759 cm^{-1} and the band at approximately 1081 cm^{-1}, corresponding to C – O – C stretching (Fig. S2a). Additionally, PLA/OFI membranes displays a band at 1598 cm^{-1}, and PLA/LIG ones are characterized by a band at 1510 cm^{-1} (Fig. S2a'). The band at 1598 and 1510 cm^{-1} can be attributed to lignin, in particular to its aromatic skeletal vibration (C = C) [36]. These results reasonably

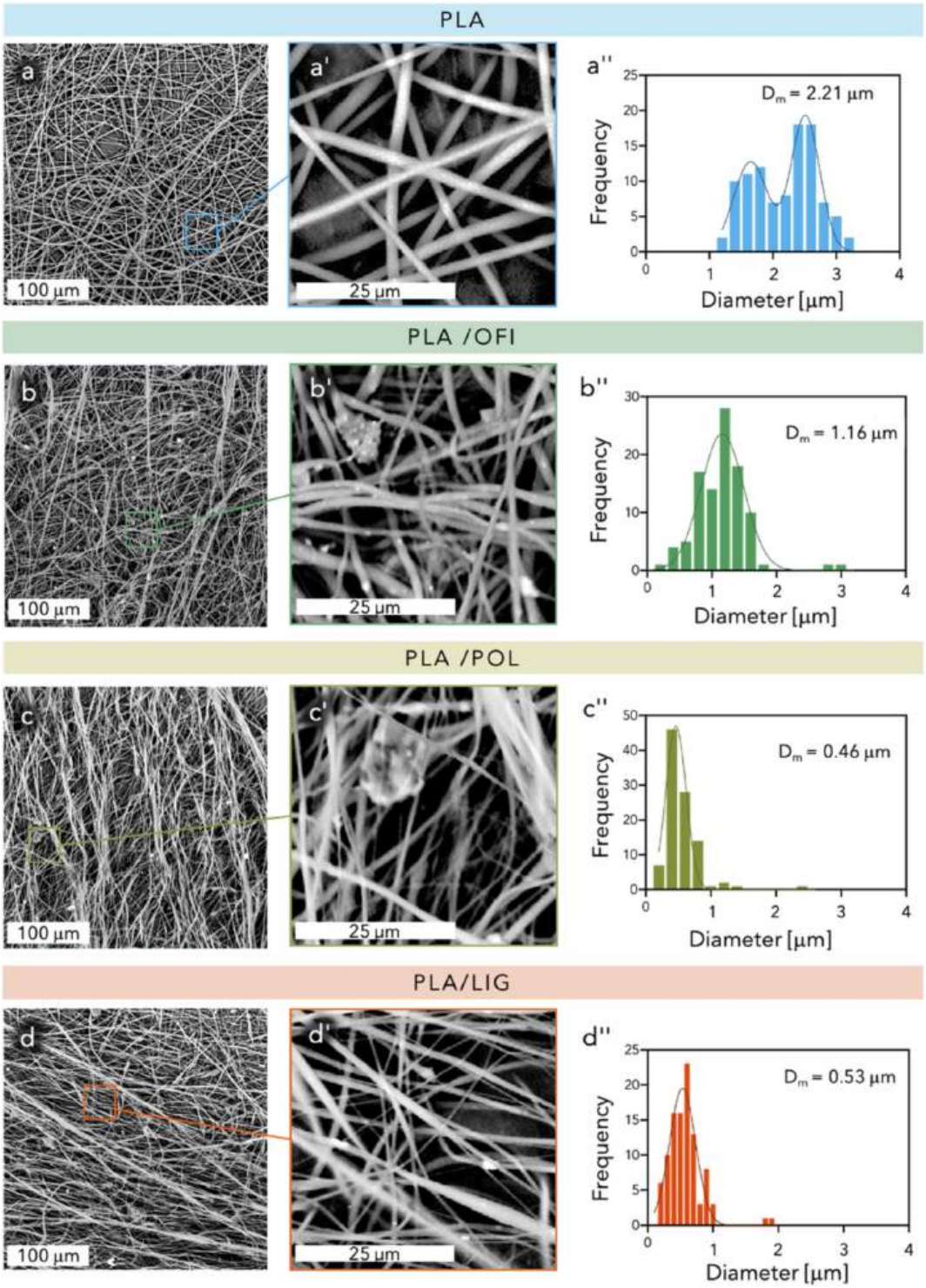

Fig. 5. SEM images, relative insets and fibers diameter distribution of PLA (a, a', a''), PLA/OFI (b, b', b''), PLA/POL (c, c', c'') and PLA/LIG (d, d', d'') membranes respectively.

confirm that OFI and LIG particles are embedded in the PLA fibers, as already observed in Fig. 5b and d, respectively. The contribution of lignin seems to be less evident in PLA/POL, probably due to the larger dimension of POL particles, which makes it more difficult to embed them in the fibers, as suggested by observing the morphology of the membrane (Fig. 5b).

Tensile tests were performed on the membranes, and elastic modulus (E, Fig. S3a), tensile strength (TS, Fig. S3b) and elongational at break (EB, Fig. S3c) are reported for all the systems. Adding the natural fillers leads to an increase in E and a corresponding decrease in TS and EB for all the composite membranes. This behaviour can be attributed to the presence of OFI, POL and LIG fillers in/on the PLA fibers. These rigid fillers enhance the overall stiffness of the composite membranes, as evidenced by the higher modulus. However, their presence also introduces potential weakness points, resulting in a reduction of the tensile strength and elongation at break. Moreover, these variations are more pronounced in PLA/POL and PLA/LIG membranes due to their smaller fibers diameter [37]. However, the obtainment of small fibers is

crucial for achieve membranes with high filtration performances. Nonetheless, the results suggest that the mechanical properties of all the composite membranes are compatible with air filtration applications [5,7,21].

3.5. Electroactivity evaluation

It is extensively reported in the scientific literature that the enhancement of electroactivity of the filtering membranes increase the removal efficiency of PM, especially for PM_1, due to the electrostatic trapping [38–40]. Moreover, the increase of electrostatic attraction is also an effective method for minimizing pressure drop [41]. Has been proved that the presence of lignin in PLA fibers enhances the electrostatic attraction of the composite membrane due to lignin dielectric properties [42]. As is possible to notice in Fig. 6, the addition of POL and especially LIG particles markedly enhances the electrostatic absorption capabilities of the membranes. More in detail, pure PLA membranes exhibit slight electrostatic properties (Fig. 6a and Video 1), characteristics of the material itself [19], and PLA/OFI (Fig. 6b and Video 2) showed electrostatic behaviour comparable to pure PLA one. On the contrary, PLA/POL (Fig. 6c and Video 3) and even more PLA/LIG (Fig. 6d and Video 4), reveal excellent electrostatic adsorption capability. The photos of the membranes surfaces after the electrostatic test are shown in Fig. 6e.

The enhanced electrostatic properties of PLA/POL and PLA/LIG membranes can be attributed to the presence of lignin that significantly amplifies the electrostatic charge of the PLA membranes. This phenomenon is due to lignin's inherent capacity to contribute to higher charge density within the polymer matrix. POL containing membranes also exhibit elevated electrostatic properties, due to its higher lignin content compared to OFI one.

3.6. Filtration performances and mechanism of PLA composites membranes

Air filtration efficiency of neat PLA and PLA composite membranes on PM_1 and PM_3 generated from the incense burning were investigated using a self-built filtration device at an airflow rate of 10, 32, 65 and 85 L/min, and the results are reported in Fig. 7(a, a'). The pressure drop and the quality factor of the fibrous membranes are shown in Fig. 7b and c, respectively. From Fig. 7(a, a') it is possible to notice that filtration efficiency of the pure PLA membrane decreases from 85.5 % to 80.3 % for PM_1, and from 88.3 % to 82.7 % for PM_3, as the flow rate increased from 10 to 85 L/min.

A similar behaviour can be noted for PLA/OFI membrane with the difference that filtration efficiencies generally increase of about 12 %, reasonably due to the smaller fibers diameters of this latter membrane if compared to pure PLA one. In contrast to this behaviour, the filtration efficiencies of PLA/POL and PLA/LIG membranes remain almost stable with the flow rate increasing, potentially due to the mitigating effect given by the increase of the electrostatic attraction effect of the membrane on increase the flow rates [19]. In general, the addition of natural fillers leads to an increase in filtration efficiency for all PM dimensions if compared to neat PLA. Regarding 32 L/min flow rate and particulates smaller than 1 μm (PM_1), the filtration efficiency increases from 84.6 % of neat PLA to 95.4 %, 97.2 % and 98.5 % of PLA/OFI, PLA/POL and PLA/LIG, respectively. Moreover, with particulate of 3 μm (PM_3), PLA/OFI, PLA/POL, and PLA/LIG display filtration efficiencies of 97.2 %, 99.4 %, 99.6 %.

The decrease in fibers diameters, the presence of natural particles, and the increase of electrostatic attraction allowed PLA/POL and PLA/LIG to achieve the highest filtration efficiency and the lowest pressure drop. The existence of electrostatic interaction between the fibers of PLA/POL and PLA/LIG membranes and PM, in fact, leads to a remarkable increase in removal efficiency, if compare to PLA/OFI membrane one, due to its capacity to strongly attract particles nearby the fibers, especially for fine particles [3].

From Fig. 7b it is possible to notice that the pressure drop of the membranes decreases when natural fillers were added. At flow rate of 32 L/min, the pressure drops of PLA/OFI, PLA/POL, and PLA/LIG were 104, 84, 76 Pa, respectively, while for pure PLA membrane pressure drop of 138 Pa were registered. The presence of the natural particles in

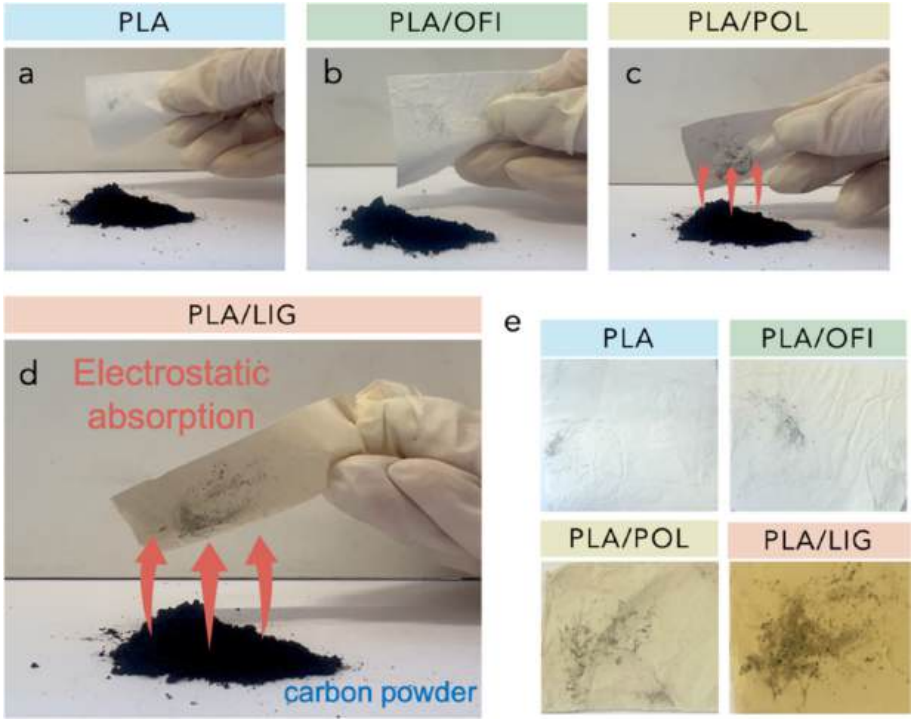

Fig. 6. Frames of digital videos showing carbon powder adsorbed on PLA (a), PLA/OFI (b), PLA/POL (c) and PLA/LIG (d) by electrostatic interactions and relative digital photograph of the membranes after the test (e).

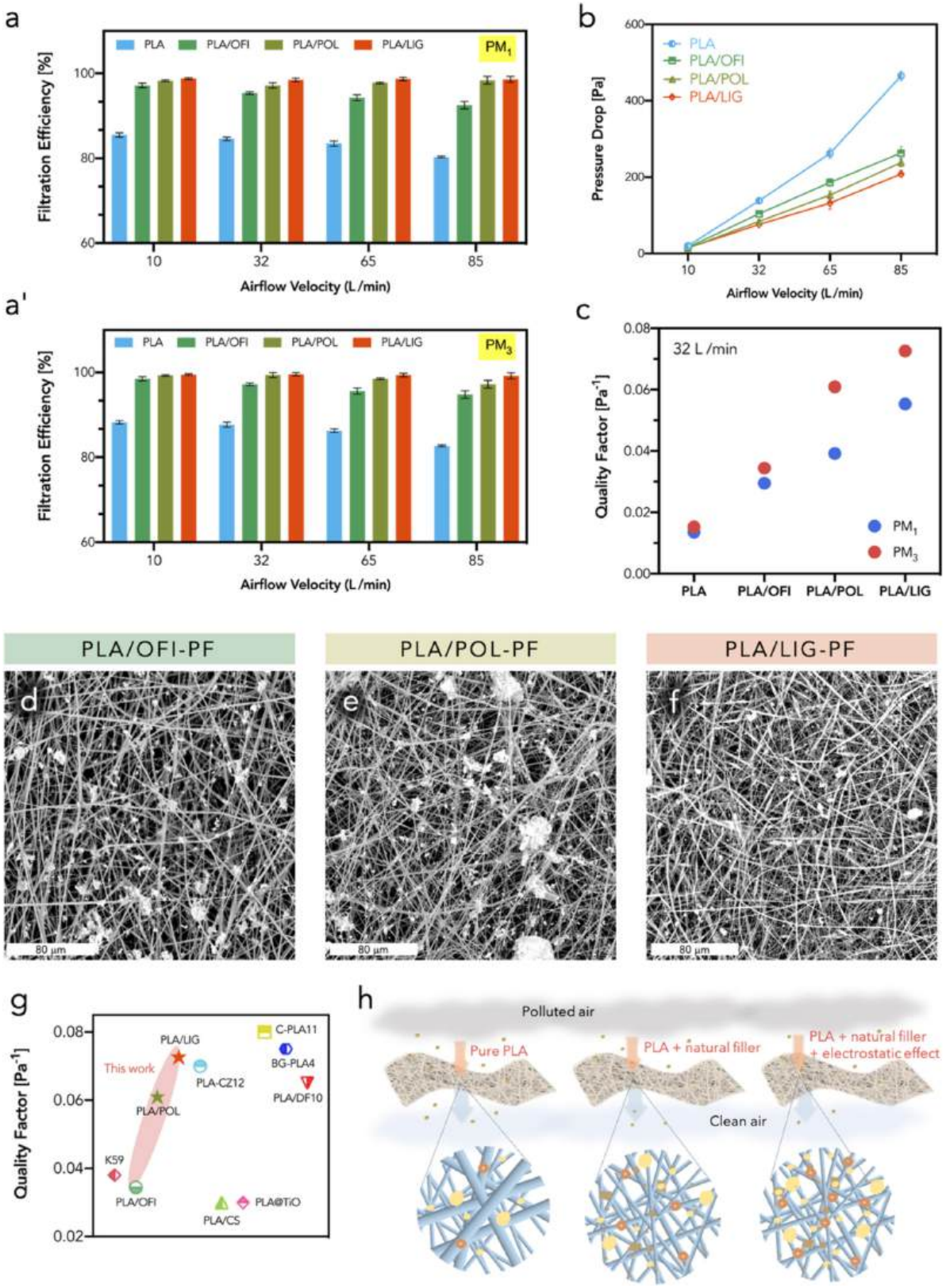

Fig. 7. Filtration performances of the composite membranes: filtration efficiency (Eq. 1) at different airflow rate for PM_1 (a) and PM_3 (a'); pressure drop at different airflow rate (b). Quality factor (Eq. 2) of the electrospun membranes for PM_1 and PM_3 (c). SEM images of (d) PLA/OFI, (e) PLA/POL, (f) PLA/LIG membranes after the filtration test (Post Filtration). Comparison of the QF values of this work with commercial filters and other PLA-based membranes under airflow velocity of 32 L/min (g). PMs capture mechanism (h).

and on the fibers surface less compaction of the membrane and induce fibers roughness, facilitating air passage and leading to an air slip effect that further decrease pressure drops.

Thanks to these behaviours, for PM_3, quality factors of 0.061 and 0.073 are obtained for PLA/POL and PLA/LIG, respectively at flow rate of 32 L/min (see Fig. 7c). According to the SEM images (Fig. 5), the addition of natural fillers decreases fibers diameter and increases their surface roughness, creating protrusions on the fibers surface, which improves the physical interception of particles by increasing the collision probability between particulates and fibers (Fig. 7d-f). This behaviour can be easily observed for PLA/OFI (Fig. 7d) and for PLA/POL (Fig. 7e) in which this effect is further enhanced by the presence of the large POL particles set on the fibers, which act as accumulation points for the particulate.

The QFs of the produced PLA composites membranes, especially for PLA/POL and PLA/LIG, are extremely encouraging when compared to commercial filters and other PLA-based composite membranes reported in the scientific literature [5,19–21,38,43], as can be observed in Fig. 7g. These results are obtained due to the involvement of different filtration mechanisms. Generally, interception, inertial impaction, sieving and Brownian diffusion can occur during air filtration [3]. As depicted in Fig. 7h, the structure of pure PLA membrane is characterized by larger fibers that create a compact structure and low electrostatic attraction (intrinsic characteristic of the material) that allow to obtain quite good filtration efficiency but also very high pressure drop due to the difficulty of airflow passing through it. On the contrary, the presence of fibers with nearly nanometric diameters in PLA/OFI, PLA/POL and PLA/LIG membranes increases the likelihood of particulates colliding with the fibers as they follow the airflow lines. Nanofibers, due to their smaller diameter, offer a significantly larger surface area compared to microfibers, which directly enhances the filtration performance. Interception, in fact, is recognized as primary filtration mechanism. Moreover, the smaller fibers diameters also enable Brownian diffusion to become more effective for capturing fine particulates. Additionally, the presence of natural filler particles embedded in and on the fibers, induce roughness, further enhances the probability of particle collisions and contextually leads to an air slip effect, which allows for easier airflow passage, that reduce pressure drops. Moreover, if the fibers are electrostatically charged, as in the case of PLA/POL and PLA/LIG (see Fig. 7h), it becomes possible to attract nearby particles that do not directly collide with the fibers, securely trapping them on the fibers surface [44,45]. This electrostatic effect is particularly effective for smaller particulates (PM_1), which are more difficult to capture through mechanical filtration alone. Especially for the PLA/POL and PLA/LIG membranes, the smaller fibers diameters and increased surface roughness create an optimal balance, where fibers arrangement is good enough to minimize airflow resistance, while the presence of natural fillers maintains effective particulate capture through a combination of electrostatic attraction and physical interception. The combination of these mechanisms - physical interception, inertial impaction, sieving, Brownian diffusion, and electrostatic attraction - ensures high filtration efficiency and low pressure drop for the PLA/POL and PLA/LIG membranes.

3.7. Stability of the composite membranes

The membranes were also tested to evaluate their stability, i.e. to verify eventual changes of filtration efficiency across different environmental conditions, including UV irradiation (Fig. 8). In particular, the filtration efficiency was evaluated at different relative humidity levels and temperatures to simulate possible different application scenarios. The filtration efficiency of PM_1 and PM_3 particles for all the membranes were tested at flow rate of 32 L/min. As it is possible to observe in Figs. 8 a and b, across the different membranes, the filtration efficiency remains relatively stable with increasing humidity, particularly for the composite membranes (PLA/OFI, PLA/POL, and PLA/LIG), that maintain high filtration efficiency levels, close to or above 97 % for both PM_1 and PM_3 particles for all humidity levels tested. More in detail, when the humidity is less than 60 %, the filtration efficiency of all the membranes remains almost unchanged for both PM_1 and PM_3. On the contrary, when the humidity increases to 80 %, the filtration efficiency of the PLA/POL and PLA/LIG membranes, for PM_1, slight decreases reasonably due to electrostatic dissipation that can occur at high humidity levels, as already observed in similar systems [38]. However, the filtration efficiency values remain significantly higher if compared with those of pure PLA. The decrease in filtration efficiency of the fibers membrane in high-humidity environments can be attributed to polar water molecules that were able to play a part of carrier for movable charges, resulting in decreased electret stability of the membranes. In high-humidity conditions, in fact, the electrostatic effect diminishes, reducing the membrane's ability to efficiently trap particulate matter [46]. This behaviour is more severe for PM_1 since are the most affected from the electrostatic attractive force. For PM_3, the filtration efficiency is almost insensitive to humidity variations (Fig. 8a) since the dominant filtration mechanism in this case is mechanical interception of the particulate matter thus the electroactivity variation did not influenced the membranes performances [44]. Similarly, temperature variation (Fig. 8 c and b) has a very small impact on the filtration efficiency of PM_1 and it has almost no effect on the filtration efficiency of PM_3. The composite membranes exhibit high and consistent filtration efficiency across the temperature range of 15 °C to 35 °C. These behaviours demonstrate that the composite membranes, particularly PLA/POL and PLA/LIG, provide superior and consistent filtration performance under varying environmental conditions, making them suitable both for indoor and outdoor applications.

The presence of plant-based fillers in PLA fibers can provide UV protection, preserving the membranes structure when exposed to sunlight [21]. To assess the resistance of the composite membranes to UV radiation, their UV transmittance was evaluated, and their morphology after 2 h of exposure to a UV lamp was investigated. The energy radiated for 1 h is equivalent to absorbing ultraviolet energy for 75–184 days under natural conditions [21]. The UV transmittance of the membranes and their morphology after UV irradiation are reported in Fig. 8e-i.

The composite membranes, especially PLA/LIG one, show extremely low UV transmittance in UVA (320–400 nm) spectrum (Fig. 8e, e'). Lignin powder, in fact, contains phenol, ketone, and other chromophores that act as UV-absorbing functional groups [47]. Similarly, also *Opuntia Ficus Indica* [48] and *Posidonia Oceanica* [49] contain flavonoids and phenolic compounds that contributes to their UV protective properties by absorbing UV radiation.

After 2 h of exposure to the UV lamp, neat PLA fibers (Fig. 8f) exhibit a notable wavy morphology. This structural alteration can be reasonably attributed UV lamp irradiation. On the other hand, PLA/OFI (Fig. 8g) and PLA/LIG (Fig. 8i) fibers remain almost unchanged after UV exposure. These results suggest that the inclusion of *Opuntia Ficus Indica* and lignin fillers in PLA fibers may provide some term of UV protection to the membranes. Interestingly, PLA/POL fibers show more waviness (Fig. 8h) if compared to their unexposed structure. This may suggest that while the addition of POL powder could reduce the extent of degradation, it does not completely prevent it, reasonably because POL particles are not well embedded in the fibers.

The UV resistance of PLA/OFI and PLA/LIG membranes were evaluated also after 4 and 8 h of accelerated UV exposures to test if them can resist longer periods of ultraviolet radiation [10] and SEM analysis were performed on them (Fig. S4). After 4 h of UV lamp exposure, the PLA/OFI membranes start to show signs of fiber modification, appearing wavier (Fig. S4a). After 8 h of exposure, the fibers are completely altered, exhibiting a highly deformed and extremely compact structure (Fig. S4b), unsuitable for the application. PLA/LIG membranes withstand UV exposure well for up to 4 h, maintaining an almost unaltered structure (Fig. S4c). However, after 8 h, the fibers undergo slight waviness and fragmentation, resulting in a compacted structure (Fig. S4d) that is no longer suitable for filtration application.

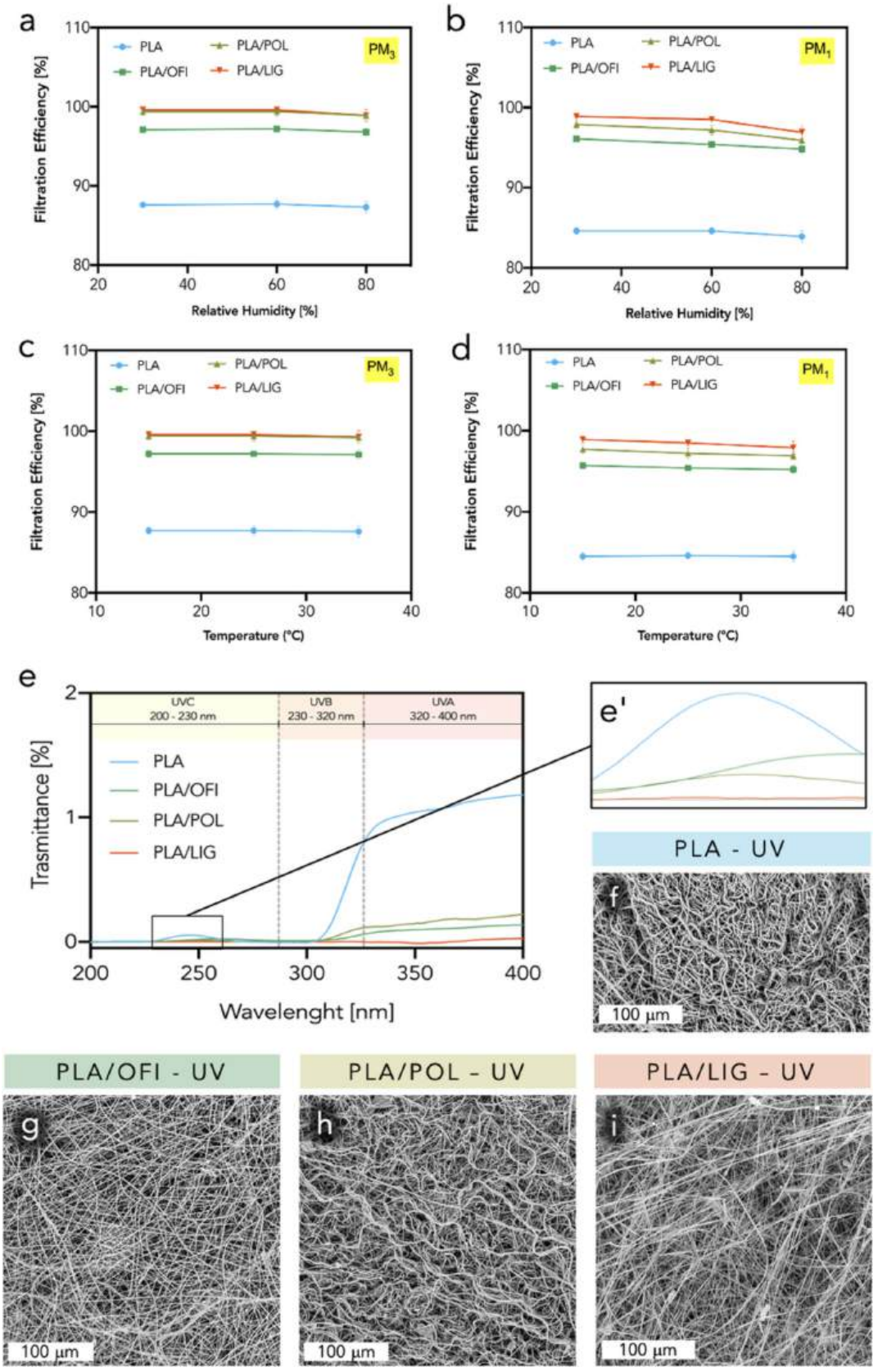

Fig. 8. Filtration efficiency of the composite membranes at different relative humidity for PM_3 (a) and PM_1 (b) and at different temperature for PM_3 (c) and PM_1 (d). Transmittance UV spectrum (e, e') and SEM images of PLA (f), PLA/OFI (g), PLA/POL (h), PLA/LIG (i) membranes after 2 h exposure to UV lamp.

3.8. Reusability of the composite membranes

To evaluate their reusability, the composite fibrous membranes were washed in a water/ethanol mixture and their filtration efficiency and pressure drop was tested for five cycles and reported in Fig. 9a and Fig. S5, respectively. Results revealed that pressure drops remain fairly constant up to five cycles, while significant changes in filtration performance of the membranes occur only after the second cycle. Specifically, the filtration efficiency remains relatively stable up to the second cycle, with minimal variation, for all the composites membranes. However, starting from the third cycle, a slight but significant reduction in filtration efficiency was observed, especially for PLA/POL and PLA/LIG membranes. This behaviour can be reasonably ascribable to the loss of the fibers' electrostatic properties [14]. Moreover, a progressive reduction in the filtration efficiency of all membrane was observed from cycle 3 to cycle 5. The washing cycles, actually, do not significantly damage the fibrous structure which remain almost unchanged as observed from SEM images in Fig. 9b-e. Moreover, after five washing cycles, the membranes showed no signs of filler detachment, demonstrating strong bonding between the natural fillers and PLA, as well as the stability of the membranes under repeated use. However, minor damage caused by handling the membranes during the filtering and washing processes gradually affect their filtration performance.

The membrane was tested over five cycles as the reduction in filtration efficiency observed within this period remains relatively small but could still be relevant for certain applications. While the performance decrease is minor, it may affect overall effectiveness in applications requiring consistently high filtration efficiency. Considering the membrane's sustainability and biodegradability, replacing it with a new one after five cycles is necessary to maintain optimal performance.

After five washing cycles, the mechanical properties of the composite fiber membranes were evaluated. All the membranes exhibited a slight decrease in E and TS, while a non-significant variation in EB was observed (Fig. S6). This behaviour is reasonably attributable to minor damage caused by handling the membranes during the filtering and washing processes. However, the fiber structure remained mostly preserved, suggesting that the washing procedure itself did not significantly impact the integrity of the membranes as it is possible to notice from SEM images (Fig. 9b-e).

4. Conclusions

In this study, stable, reusable and UV-resistant bio-composite fibrous membranes were successfully fabricated through electrospinning. The composite dispersions were prepared by adding 10 wt% of *Opuntia Ficus Indica* (OFI), *Posidonia Oceanica Leaves* (POL) or lignin (LIG) powders to the PLA solution. The PLA/POL and PLA/LIG membranes exhibited a significant decrease in fiber diameter, attributable to the increased conductivity of the solutions. Additionally, the presence of lignin in the membranes enhanced their electroactivity. The mechanical properties of all the composite membranes are compatible with air filtration applications. The PLA/OFI, PLA/POL and PLA/LIG composite membranes exhibited high filtration performances for PM_3 at a flow rate of 32 L/min, with filtration efficiencies of 97.2 %, 99.4 %, 99.6 %, and pressure drops of 114, 103, 105 Pa, respectively. For PLA/POL and PLA/LIG membranes the contextual decrease in fibers diameters and increase in electrostatic attraction were the key factors to enhance filtration performances of the membranes. The composite membranes demonstrated satisfactory stability maintaining good filtration efficiency across different relative humidity and temperature conditions. It was also demonstrated that the inclusion of OFI and LIG powders in PLA fibers provides some term of UV protection to the filtering membranes. PLA/OFI and PLA/LIG membranes remained almost unchanged after 4 h of accelerated UV irradiation. Moreover, the composite membranes demonstrated the ability to be reused for at least five washing cycles while maintaining their fibrous structure and preserving good filtration efficiency. Therefore, the PLA/OFI, PLA/POL and PLA/LIG membranes prepared in this study exhibit enormous potential for air filtration

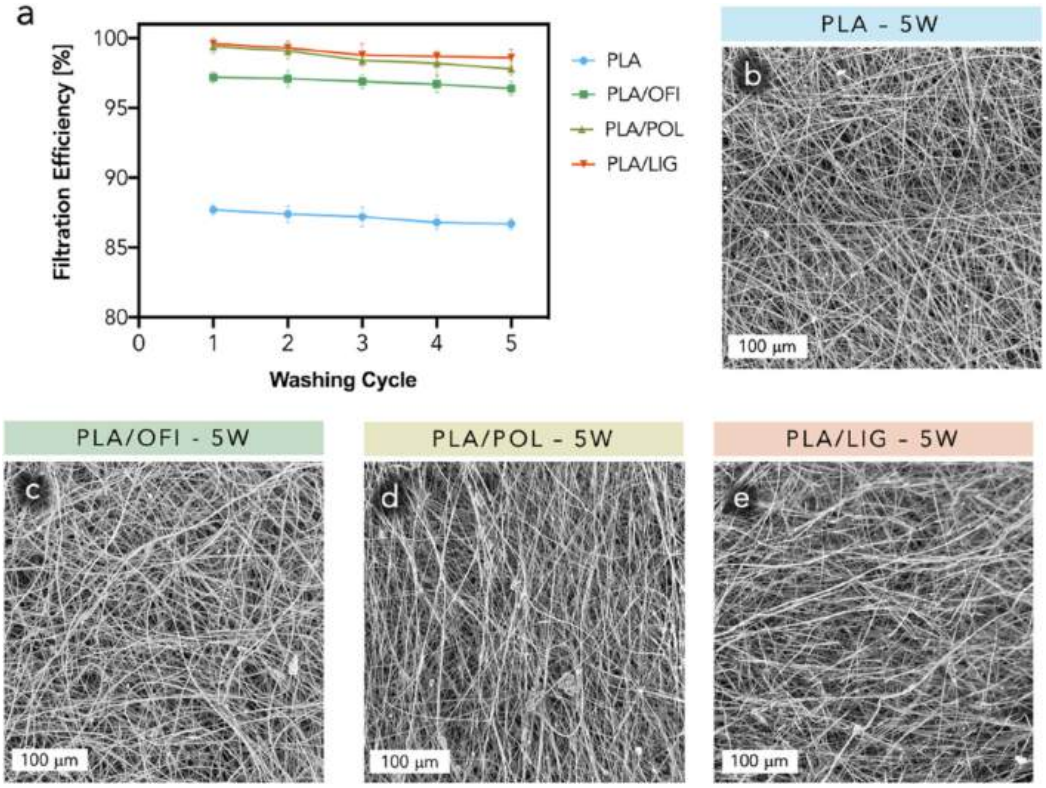

Fig. 9. (a) Reusability of the composite membranes: filtration efficiency after five cycles. SEM images of PLA (b), PLA/OFI (c), PLA/POL (d) and PLA/LIG e) membranes after five cycles of washing and filtration testing.

application both for indoor and outdoor filtering devices.

Supplementary data to this article can be found online at https://doi.org/10.1016/j.susmat.2024.e01146.

CRediT authorship contribution statement

Roberto Scaffaro: Writing – review & editing, Validation, Supervision, Resources, Project administration, Funding acquisition. **Maria Clara Citarrella:** Writing – review & editing, Writing – original draft, Visualization, Validation, Software, Methodology, Investigation, Formal analysis, Data curation, Conceptualization.

Declaration of competing interest

The authors declare no conflict of interest.

Data availability

Data will be made available on request.

Acknowledgement

We are grateful for financial support of SiciliAn MicronanOTecH Research And Innovation CEnter "SAMOTHRACE" (MUR, PNRR-M4C2, ECS_00000022), spoke 3 - Università degli Studi di Palermo "S2-COMMs - Micro and Nanotechnologies for Smart & Sustainable Communities and MICS (Made in Italy – Circular and Sustainable) Extended Partnership and received funding from the European Union Next-GenerationEU (PIANO NAZIONALE DI RIPRESA E RESILIENZA (PNRR) – MISSIONE 4 COMPONENTE 2, INVESTIMENTO 1.3 – D.D. 1551.11-10-2022, PE00000004).

References

[1] S. Ren, M. Du, W. Bu, T. Lin, Assessing the impact of economic growth target constraints on environmental pollution: does environmental decentralization matter? J. Environ. Manag. 336 (2023) 117618 https://doi.org/10.1016/J.JENVMAN.2023.117618.

[2] E. Madonia, A. Di Vincenzo, A. Pettignano, R. Scaffaro, E.F. Gulino, P. Conte, P. Lo Meo, Composite RGO/Ag/nanosponge materials for the photodegradation of emerging pollutants from wastewaters, Materials 17 (2024) 2319, https://doi.org/10.3390/MA17102319.

[3] R. Scaffaro, M.C. Citarrella, R. Scaffaro, M.C. Citarrella, Nanofibrous polymeric membranes for air filtration application: a review of Progress after the COVID-19 pandemic, Macromol. Mater. Eng. 308 (2023) 2300072, https://doi.org/10.1002/MAME.202300072.

[4] Z. Lou, L. Wang, K. Yu, Q. Wei, T. Hussain, X. Xia, H. Zhou, Electrospun PVB/AVE NMs as mask filter layer for win-win effects of filtration and antibacterial activity, J. Membr. Sci. 672 (2023) 121473, https://doi.org/10.1016/J.MEMSCI.2023.121473.

[5] C. Zhang, J. Sun, S. Lyu, Z. Lu, T. Li, Y. Yang, B. Li, H. Han, B. Wu, H. Sun, D. Li, J. Huang, D. Sun, Poly(lactic acid)/artificially cultured diatom frustules nanofibrous membranes with fast and controllable degradation rates for air filtration, Adv. Compos. Hybrid Mater. 5 (2022) 1221–1232, https://doi.org/10.1007/S42114-022-00474-7.

[6] Y. Kara, K. Molnár, A review of processing strategies to generate melt-blown nano/microfiber mats for high-efficiency filtration applications, J. Ind. Text. 51 (2022) 137S–180S, https://doi.org/10.1177/15280837211019488.

[7] M. Jafari, E. Shim, A. Joijode, Fabrication of poly(lactic acid) filter media via the meltblowing process and their filtration performances: a comparative study with polypropylene meltblown, Sep. Purif. Technol. 260 (2021) 118185, https://doi.org/10.1016/J.SEPPUR.2020.118185.

[8] V. Aryan, D. Maga, P. Majgaonkar, R. Hanich, Valorisation of polylactic acid (PLA) waste: a comparative life cycle assessment of various solvent-based chemical recycling technologies, Resour. Conserv. Recycl. 172 (2021) 105670, https://doi.org/10.1016/J.RESCONREC.2021.105670.

[9] K. Rafiee, G. Kaur, S.K. Brar, Recycling and reuse issues of PLA and PLA/cellulose composites, Polylactic Acid Based Nanocell. Cell. Compos. (2022) 265–276, https://doi.org/10.1201/9781003160458-13.

[10] W. Ma, Y. Ding, M. Zhang, S. Gao, Y. Li, C. Huang, G. Fu, Nature-inspired chemistry toward hierarchical superhydrophobic, antibacterial and biocompatible nanofibrous membranes for effective UV-shielding, self-cleaning and oil-water separation, J. Hazard. Mater. 384 (2020) 121476, https://doi.org/10.1016/J.JHAZMAT.2019.121476.

[11] Y. Bian, C. Zhang, H. Wang, Q. Cao, Degradable nanofiber for eco-friendly air filtration: Progress and perspectives, Sep. Purif. Technol. 306 (2023) 122642, https://doi.org/10.1016/J.SEPPUR.2022.122642.

[12] R. Scaffaro, E.F. Gulino, M.C. Citarrella, Biodegradable membrane with high porosity and hollow structure obtained via electrospinning for oil spill clean-up application, J. Polym. Environ. 31 (2023) 3965–3981, https://doi.org/10.1007/S10924-023-02876-0.

[13] R. Scaffaro, L. Settanni, E.F. Gulino, Release profiles of carvacrol or chlorhexidine of pla/graphene nanoplatelets membranes prepared using electrospinning and solution blow spinning: a comparative study, Molecules 28 (2023) 1967, https://doi.org/10.3390/MOLECULES28041967.

[14] C. Wang, X. He, G. Zhu, X. Li, X. Zhu, R. Chen, S. Tian, X. Li, J. Zhu, J. Shao, J. Gao, G.J. Zhong, H. Xu, Extreme orientation of Stereocomplexed poly(lactic acid) induced ultrafine electroactive nanofibers for respiratory healthcare and intelligent diagnosis, ACS Sustain. Chem. Eng. 12 (2024) 9290–9300, https://doi.org/10.1021/ACSSUSCHEMENG.4C02720.

[15] G. Zhu, C. Wang, T. Yang, N. Gao, Y. Zhang, J. Zhu, X. He, J. Shao, S. Li, M. Zhang, S. Zhang, J. Gao, H. Xu, Bio-inspired gradient poly(lactic acid) nanofibers for active capturing of PM0.3 and real-time respiratory monitoring, J. Hazard. Mater. 474 (2024) 134781, https://doi.org/10.1016/J.JHAZMAT.2024.134781.

[16] X. Song, X. He, M. Tang, C. Wang, Y. Zhang, X. Li, T. Li, L. Ke, X. Li, M. Zhang, S. Zhang, H. Xu, Multi-protection from microbial and PM pollutants by humidity-resistant, breathable and self-charging nanofibrous membranes, ACS Sustain. Chem. Eng. 12 (2024) 12216–12225, https://doi.org/10.1021/ACSSUSCHEMENG.4C04333.

[17] T. Yang, K. Xu, G. Zhu, Y. Zhang, X. Zhu, X. Li, J. Shao, J. Zhu, M. Zhang, X. He, S. Zhang, Y. Zhu, J. Gao, G.J. Zhong, H. Xu, Hierarchically structured poly(lactic acid) nanofibers by organic–inorganic nanohybridization strategy towards efficient PM removal and respiratory monitoring, Sep. Purif. Technol. 354 (2025) 128886, https://doi.org/10.1016/J.SEPPUR.2024.128886.

[18] Y. Lou, B. Wang, J. Ma, R. Yang, X. Jin, F. Liu, M. Yang, Z. Sun, X. Li, X. Zhang, A versatile electrospun polylactic acid nanofiber membrane integrated with halloysite nanotubes for indoor air purification, disinfection, and photocatalytic degradation of pollutants, Sep. Purif. Technol. 323 (2023) 124371, https://doi.org/10.1016/J.SEPPUR.2023.124371.

[19] L. Jiang, X. Zhu, J. Li, J. Shao, Y. Zhang, J. Zhu, S. Li, L. Zheng, X.P. Li, S. Zhang, H. Li, G.J. Zhong, H. Xu, Electroactive and breathable protective membranes by surface engineering of dielectric nanohybrids at poly(lactic acid) nanofibers with excellent self-sterilization and photothermal properties, Sep. Purif. Technol. 339 (2024) 126708, https://doi.org/10.1016/J.SEPPUR.2024.126708.

[20] T. Yang, X. Zhu, Y. Zhang, L. Ke, J. Zhu, R. Huang, S. Li, Y. Zhu, S. Zhang, G. J. Zhong, H. Xu, Nanopatterning of beaded poly(lactic acid) nanofibers for highly electroactive, breathable, UV-shielding and antibacterial protective membranes, Int. J. Biol. Macromol. 260 (2024) 129566, https://doi.org/10.1016/J.IJBIOMAC.2024.129566.

[21] J. Ge, D. Han, S. Li, J. Li, S. Hong, C. Wang, P. Hu, S. Ramakrishna, Y. Liu, Electrospun membrane of PLA/calendula with improved UV protection and stable filtration performance, Sep. Purif. Technol. 344 (2024) 127310, https://doi.org/10.1016/J.SEPPUR.2024.127310.

[22] E.F. Gulino, M.C. Citarrella, A. Maio, R. Scaffaro, An innovative route to prepare in situ graded crosslinked PVA graphene electrospun mats for drug release, Compos. Part A Appl. Sci. Manuf. 155 (2022) 106827, https://doi.org/10.1016/J.COMPOSITESA.2022.106827.

[23] W. Cao, M. Zhang, W. Ma, C. Huang, Multifunctional electrospun nanofibrous membrane: an effective method for water purification, Sep. Purif. Technol. 327 (2023) 124952, https://doi.org/10.1016/J.SEPPUR.2023.124952.

[24] M.A. Abdulhamid, K. Muzamil, Recent progress on electrospun nanofibrous polymer membranes for water and air purification: a review, Chemosphere 310 (2023) 136886, https://doi.org/10.1016/J.CHEMOSPHERE.2022.136886.

[25] Y. Deng, T. Lu, X. Zhang, Z. Zeng, R. Tao, Q. Qu, Y. Zhang, M. Zhu, R. Xiong, C. Huang, Multi-hierarchical nanofiber membrane with typical curved-ribbon structure fabricated by green electrospinning for efficient, breathable and sustainable air filtration, J. Membr. Sci. 660 (2022) 120857, https://doi.org/10.1016/J.MEMSCI.2022.120857.

[26] H. Chakhtouna, H. Benzeid, N. Zari, A. El Kacem Qaiss, R. Bouhfid, Recent advances in eco-friendly composites derived from lignocellulosic biomass for wastewater treatment, Biomass Convers. Biorefinery 2022 (1) (2022) 1–27, https://doi.org/10.1007/S13399-022-03159-9.

[27] R. Scaffaro, E.F. Gulino, M.C. Citarrella, Multifunctional 3D-printed composites based on biopolymeric matrices and tomato plant (Solanum lycopersicum) waste for contextual fertilizer release and cu(II) ions removal, Adv. Compos. Hybrid Mater. 7 (2024) 1–16, https://doi.org/10.1007/S42114-024-00908-4.

[28] R. Scaffaro, M.C. Citarrella, E.F. Gulino, Opuntia Ficus Indica based green composites for NPK fertilizer controlled release produced by compression molding and fused deposition modeling, Compos. Part A Appl. Sci. Manuf. 159 (2022) 107030, https://doi.org/10.1016/J.COMPOSITESA.2022.107030.

[29] B.G.K. Steiger, Z. Zhou, Y.A. Anisimov, R.W. Evitts, L.D. Wilson, Valorization of agro-waste biomass as composite adsorbents for sustainable wastewater treatment, Ind. Crop. Prod. 191 (2023) 115913, https://doi.org/10.1016/J.INDCROP.2022.115913.

[30] L. Li, Y. Gao, G. Nie, X. Yan, S. Wang, T. Zhang, S. Ramakrishna, Y.Z. Long, W. Han, Biodegradable poly (L-lactic acid) fibrous membrane with ribbon-structured fibers and ultrafine nanofibers enhances air filtration performance, Small (2024) 2402317, https://doi.org/10.1002/SMLL.202402317.

[31] R. Scaffaro, A. Maio, E.F. Gulino, Hydrolytic degradation of PLA/Posidonia Oceanica green composites: a simple model based on starting morpho-chemical

properties, Compos. Sci. Technol. 213 (2021) 108930, https://doi.org/10.1016/J.COMPSCITECH.2021.108930.
[32] M.R.V. Fontes, M.P. da Rosa, L.M. Fonseca, P.H. Beck, E. da Rosa Zavareze, A.R. G. Dias, Thermal stability, hydrophobicity and antioxidant potential of ultrafine poly (lactic acid)/rice husk lignin fibers, Braz. J. Chem. Eng. 38 (2021) 133–144, https://doi.org/10.1007/S43153-020-00083-1.
[33] N. Dalton, R.P. Lynch, M.N. Collins, M. Culebras, Thermoelectric properties of electrospun carbon nanofibres derived from lignin, Int. J. Biol. Macromol. 121 (2019) 472–479, https://doi.org/10.1016/J.IJBIOMAC.2018.10.051.
[34] C. Cocozza, A. Parente, C. Zaccone, C. Mininni, P. Santamaria, T. Miano, Chemical, physical and spectroscopic characterization of Posidonia oceanica (L.) Del. Residues and their possible recycle, Biomass Bioenergy 35 (2011) 799–807, https://doi.org/10.1016/J.BIOMBIOE.2010.10.033.
[35] R. Casasola, N.L. Thomas, A. Trybala, S. Georgiadou, Electrospun poly lactic acid (PLA) fibres: effect of different solvent systems on fibre morphology and diameter, Polymer (Guildf) 55 (2014) 4728–4737, https://doi.org/10.1016/J.POLYMER.2014.06.032.
[36] Y. Liu, T. Hu, Z. Wu, G. Zeng, D. Huang, Y. Shen, X. He, M. Lai, Y. He, Study on biodegradation process of lignin by FTIR and DSC, Environ. Sci. Pollut. Res. 21 (2014) 14004–14013, https://doi.org/10.1007/S11356-014-3342-5.
[37] T.U. Rashid, R.E. Gorga, W.E. Krause, Mechanical properties of electrospun fibers—a critical review, Adv. Eng. Mater. 23 (2021), https://doi.org/10.1002/ADEM.202100153.
[38] G. Zhu, C. Wang, T. Yang, N. Gao, Y. Zhang, J. Zhu, X. He, J. Shao, S. Li, M. Zhang, S. Zhang, J. Gao, H. Xu, Bio-inspired gradient poly(lactic acid) nanofibers for active capturing of PM0.3 and real-time respiratory monitoring, J. Hazard. Mater. 474 (2024) 134781, https://doi.org/10.1016/J.JHAZMAT.2024.134781.
[39] C. Wang, X. He, G. Zhu, X. Li, X. Zhu, R. Chen, S. Tian, X. Li, J. Zhu, J. Shao, J. Gao, G.J. Zhong, H. Xu, Extreme orientation of stereocomplexed poly(lactic acid) induced ultrafine electroactive nanofibers for respiratory healthcare and intelligent diagnosis, ACS Sustain. Chem. Eng. (2024), https://doi.org/10.1021/ACSSUSCHEMENG.4C02720.
[40] X. Song, M. Tang, C. Wang, X. Li, J. Zhu, J. Shao, S. Huang, B. Wang, X.P. Li, H. Li, H. Xu, Stereocomplexation-enhanced electroactivity of poly(lactic acid) nanofibrous membranes for long-term PM capturing and remote respiratory monitoring, ACS Sustain. Chem. Eng. 12 (2024) 3554–3564, https://doi.org/10.1021/ACSSUSCHEMENG.3C06327.
[41] Y. Wang, X. Zhang, X. Jin, W. Liu, An in situ self-charging triboelectric air filter with high removal efficiency, ultra-low pressure drop, superior filtration stability, and robust service life, Nano Energy 105 (2023) 108021, https://doi.org/10.1016/J.NANOEN.2022.108021.
[42] M.H. Wolf, N. Izaguirre, B. Pascual-José, R. Teruel-Juanes, J. Labidi, A. Ribes-Greus, Dielectric characterisation of chitosan-based composite membranes containing fractionated Kraft and organosolv lignin, React. Funct. Polym. 196 (2024) 105833, https://doi.org/10.1016/J.REACTFUNCTPOLYM.2024.105833.
[43] H. Li, Z. Wang, H. Zhang, Z. Pan, Nanoporous PLA/(chitosan nanoparticle) composite fibrous membranes with excellent air filtration and antibacterial performance, Polymers 10 (2018) 1085, https://doi.org/10.3390/POLYM10101085.
[44] M. Zhu, Y. Deng, Y. Zheng, X. Hu, W. Xu, R. Xiong, C. Huang, Tribo-charge enhanced and cellulose based biodegradable nanofibrous membranes with highly fluffy structure for air filtration and self-powered respiration monitoring systems, J. Hazard. Mater. 468 (2024) 133770, https://doi.org/10.1016/J.JHAZMAT.2024.133770.
[45] D. Lv, G. Tang, L. Chen, M. Zhang, J. Cui, R. Xiong, C. Huang, Multifunctional gas-spinning hierarchical architecture: a robust and efficient nanofiber membrane for simultaneous air and water contaminant remediation, ACS Appl. Polym. Mater. 2 (2020) 5686–5697, https://doi.org/10.1021/ACSAPM.0C00988.
[46] C. Liu, Z. Dai, B. He, Q.F. Ke, The effect of temperature and humidity on the filtration performance of electret melt-blown nonwovens, Materials 13 (2020) 4774, https://doi.org/10.3390/MA13214774.
[47] P. Santhra Krishnan, A. Salian, S. Dutta, S. Mandal, A roadmap to UV-protective natural resources: classification, characteristics, and applications, Mater. Chem. Front. 5 (2021) 7696–7723, https://doi.org/10.1039/D1QM00741F.
[48] G. Petruk, F. Di Lorenzo, P. Imbimbo, A. Silipo, A. Bonina, L. Rizza, R. Piccoli, D. M. Monti, R. Lanzetta, Protective effect of Opuntia ficus-indica L. cladodes against UVA-induced oxidative stress in normal human keratinocytes, Bioorg. Med. Chem. Lett. 27 (2017) 5485–5489, https://doi.org/10.1016/J.BMCL.2017.10.043.
[49] A.M. Mannino, C. Micheli, Ecological function of phenolic compounds from mediterranean fucoid algae and seagrasses: an overview on the genus cystoseira sensu lato and *Posidonia oceanica* (L.) Delile, J. Mar. Sci. Eng. 8 (19) (2020) 19, https://doi.org/10.3390/JMSE8010019.